



## Rapid estimation of sugar release from winter wheat straw during bioethanol production using FTIR-photoacoustic spectroscopy

Bekiaris, Georgios; Lindedam, Jane; Peltre, Clément; Decker, Stephen R.; Turner, Geoffrey B.; Magid, Jakob; Bruun, Sander

*Published in:*  
Biotechnology for Biofuels

*DOI:*  
[10.1186/s13068-015-0267-2](https://doi.org/10.1186/s13068-015-0267-2)

*Publication date:*  
2015

*Document version*  
Publisher's PDF, also known as Version of record

*Citation for published version (APA):*  
Bekiaris, G., Lindedam, J., Peltre, C., Decker, S. R., Turner, G. B., Magid, J., & Bruun, S. (2015). Rapid estimation of sugar release from winter wheat straw during bioethanol production using FTIR-photoacoustic spectroscopy. *Biotechnology for Biofuels*, 8(1), [85]. <https://doi.org/10.1186/s13068-015-0267-2>



RESEARCH ARTICLE

Open Access



# Rapid estimation of sugar release from winter wheat straw during bioethanol production using FTIR-photoacoustic spectroscopy

Georgios Bekiaris<sup>1</sup>, Jane Lindedam<sup>1</sup>, Clément Peltre<sup>1</sup>, Stephen R. Decker<sup>2</sup>, Geoffrey B. Turner<sup>2</sup>, Jakob Magid<sup>1</sup> and Sander Bruun<sup>1\*</sup>

## Abstract

**Background:** Complexity and high cost are the main limitations for high-throughput screening methods for the estimation of the sugar release from plant materials during bioethanol production. In addition, it is important that we improve our understanding of the mechanisms by which different chemical components are affecting the degradability of plant material. In this study, Fourier transform infrared photoacoustic spectroscopy (FTIR-PAS) was combined with advanced chemometrics to develop calibration models predicting the amount of sugars released after pretreatment and enzymatic hydrolysis of wheat straw during bioethanol production, and the spectra were analysed to identify components associated with recalcitrance.

**Results:** A total of 1122 wheat straw samples from nine different locations in Denmark and one location in the United Kingdom, spanning a large variation in genetic material and environmental conditions during growth, were analysed. The FTIR-PAS spectra of non-pretreated wheat straw were correlated with the measured sugar release, determined by a high-throughput pretreatment and enzymatic hydrolysis (HTPH) assay. A partial least square regression (PLSR) calibration model predicting the glucose and xylose release was developed. The interpretation of the regression coefficients revealed a positive correlation between the released glucose and xylose with easily hydrolysable compounds, such as amorphous cellulose and hemicellulose. Additionally, a negative correlation with crystalline cellulose and lignin, which inhibits cellulose and hemicellulose hydrolysis, was observed.

**Conclusions:** FTIR-PAS was used as a reliable method for the rapid estimation of sugar release during bioethanol production. The spectra revealed that lignin inhibited the hydrolysis of polysaccharides into monomers, while the crystallinity of cellulose retarded its hydrolysis into glucose. Amorphous cellulose and xylans were found to contribute significantly to the released amounts of glucose and xylose, respectively.

**Keywords:** Bioethanol production, FTIR-photoacoustic spectroscopy, Sugar release, Prediction, High-throughput assay, Pretreatment, Enzymatic hydrolysis, Advanced chemometrics

## Background

Production systems for second generation biofuels produced from lignocellulosic biomass have been evolving in the last few decades in an attempt to reduce the environmental impact and sustainability issues arising from the wide-scale production and use of conventional biofuels [1]. Lignocellulosic biomass constitutes about 50 %

of the world's biomass [2], while it has been estimated that more than  $442 \times 10^9$  L of bioethanol can be produced per year from the lignocellulosic biomass left in the fields [3]. One of the challenges for the use of lignocellulosic biomass for bioethanol production is to develop cheap and efficient pretreatment methods that disrupt the lignocellulosic complex making the cellulose more amorphous as well as removing or degrading lignin [4]. The degradation of lignin makes plant biomass more susceptible to quick hydrolysis and increases the yields of monomeric sugars necessary for bioethanol production [5]. This increase in

\* Correspondence: sab@plen.ku.dk

<sup>1</sup>Department of Plant and Environmental Sciences, Faculty of Science, University of Copenhagen, Thorvaldsensvej 40, Frederiksberg C DK-1871, Denmark

Full list of author information is available at the end of the article

the yields of monomeric sugars results in the production of larger amounts of bioethanol.

However, even after pretreatment, differences in straw from different varieties or cultivars produced under different environmental conditions are still likely to prevail [6]. To select the best cultivars, it is desirable to assess the potential for sugar release after pretreatment and hydrolysis of a large number of cultivars. For this purpose, high-throughput screening methods have been developed [7–9]. The complexity of the required pretreatment and enzymatic hydrolysis of the biomass, as well as the cost per sample, are the main limitations of these techniques [10]. Near infrared spectroscopy (NIRS) has been adopted as a rapid analysis method that can predict the sugar release upon pretreatment and hydrolysis of groups of plant biomass [11–13]. Good prediction accuracy can be achieved using this technique, but it provides limited information about the chemical components that are associated with the propensity to release sugars. The reason for this is that the near infrared (NIR) spectra mostly reflect overtones and the combination bands of the chemical bonds, which are highly overlapping [14].

A large number of literature studies have provided insights on Fourier transform infrared (FTIR) spectra interpretation [15–17]. Attenuated total reflection FTIR (ATR-FTIR) spectroscopy has been adopted in the past to determine the changes that take place during the pretreatment of wheat straw [18], as well as the transformation of cellulose during the enzymatic hydrolysis for bioethanol production [19]. ATR-FTIR has also been used, in combination with advanced chemometrics, to predict the composition of pretreated softwood [20] as well as the glucan, xylan and other polysaccharide content of straw [21]. Only a limited number of attempts have been made to apply mid-infrared spectroscopy in the prediction of fermentable sugars from pretreated biomass [16, 22, 23]; there have been no previous attempts to correlate the FTIR or Fourier transform infrared photoacoustic (FTIR-PA) spectra of non-pretreated biomass with their potential sugar release. FTIR-PAS arises from combining traditional FTIR and a photoacoustic detector (PA). The measurement of the absorbed radiation is directly proportional to the heat wave produced after the interaction of the sample with the IR radiation. In this way, the measurement remains unaffected by the redistribution of the light due to scattering effects or diffraction processes [24–26].

Therefore, the aim of the present study was to use FTIR-PAS for the characterisation of winter wheat straw and identification of chemical structures related to sugar release and to develop calibrations predicting potential sugar release from FTIR-PA spectra.

## Results and discussion

### Spectroscopic analysis

The averaged spectra of each site and variety were characterised by common peaks with slightly different absorption intensities (Fig. 1a, b). The different peaks correspond to fundamental molecular stretching and bending vibrations of different chemical groups in the samples (Table 1). The broad peak centred at  $3380\text{ cm}^{-1}$  (peak 1) can be assigned to water or lignin from wood samples, while the peak at  $2920\text{ cm}^{-1}$  (peak 2) and the shoulder at  $2850\text{ cm}^{-1}$  (peak 3) correspond to aliphatics. Ciolacu et al. [27] observed a shift in this peak from  $2900\text{ cm}^{-1}$  for pure cellulose to  $2920\text{ cm}^{-1}$  for the amorphous cellulose. In the fingerprint region ( $1800\text{--}600\text{ cm}^{-1}$ ) of the spectrum, strong absorption was observed at  $1735\text{ cm}^{-1}$  (peak 4), which, as the shoulder at  $1460\text{ cm}^{-1}$  (peak 8), correspond to xylans. The peak at  $1650\text{ cm}^{-1}$  (peak 5), which revealed a diversification in the absorption intensity, corresponds either to carboxylates or the absorbed water; therefore, the difference in the absorption intensity probably indicated different contents of carboxylates, as all samples were dried following the same procedure. The peaks at  $1600$  (peak 6) and  $1510\text{ cm}^{-1}$  (peak 7) are associated with lignin. The IR absorption at  $1429\text{ cm}^{-1}$  (peak 9) corresponds to lignin or crystalline cellulose, while the peak at  $1370\text{ cm}^{-1}$  (peak 10) can be assigned to cellulose and hemicellulose. Ciolacu et al. [27] observed a positive correlation of crystalline cellulose with both regions ( $1429$  and  $1370\text{ cm}^{-1}$ ) for various materials, while both of them seem to be absent in amorphous cellulose or replaced by a strong peak shifted at  $1400\text{ cm}^{-1}$ . The relatively strong peak that was visible at  $1320\text{ cm}^{-1}$  (peak 11) could be part of either the peak at  $1335\text{ cm}^{-1}$  observed by Pandey and Pitman [28] corresponding to the C-H vibration of cellulose, hemicellulose, lignin, or the peak at  $1310\text{ cm}^{-1}$  observed by Sills and Gossett [16] corresponding to the  $\text{CH}_2$  wagging in cellulose and hemicellulose. The relatively broad peak at  $1240\text{ cm}^{-1}$  (peak 12) could be assigned to xylans, while the peak at  $1160\text{ cm}^{-1}$  (peak 13) corresponds to cellulose and hemicellulose. According to Ciolacu et al. [27], while this peak is observed in the FTIR spectra of original cellulose, it is absent in the spectra of the amorphous form of cellulose. Both peaks at  $1111\text{ cm}^{-1}$  (peak 14) and  $1053\text{ cm}^{-1}$  (peak 15) correspond to crystalline cellulose, while the peak at  $898\text{ cm}^{-1}$  (peak 16) can be assigned to amorphous cellulose.

### Sugar release

The high-throughput pretreatment and enzymatic hydrolysis (HTPH) measurements of the samples shown in Table 2 revealed a range in the sugar yield from  $0.28$  to  $0.59\text{ g g}^{-1}$  of dry matter (dm) for total sugars,  $0.14$  to  $0.50\text{ g g}^{-1}$  dm for glucose and  $0.06$  to  $0.29\text{ g g}^{-1}$  dm for

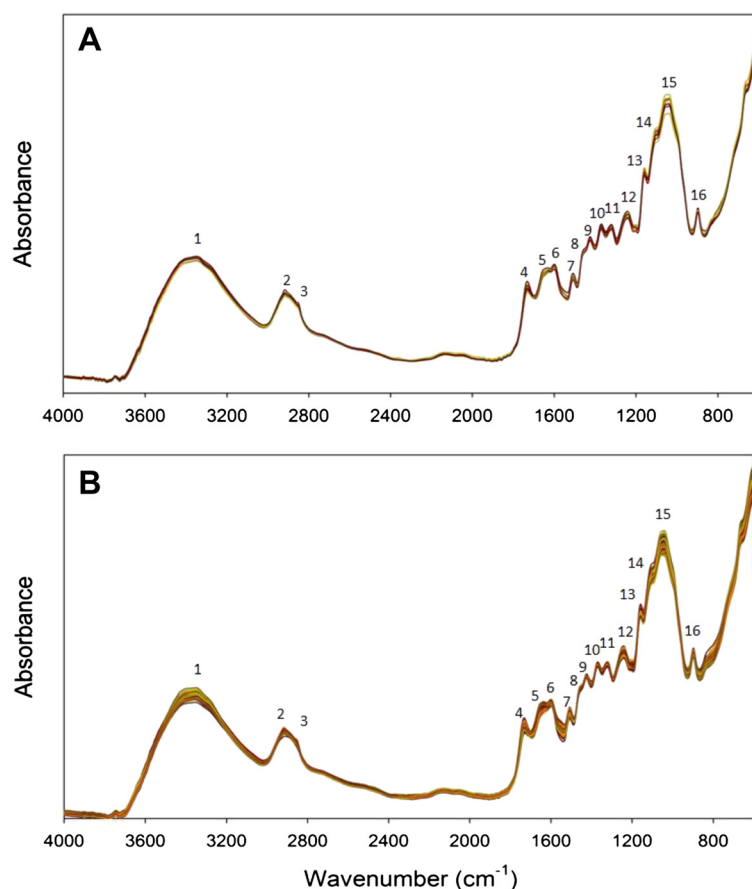


**Fig. 1** FTIR-PA spectra of winter wheat straw. **a** Spectra averaged across different locations (nine spectra). **b** Spectra averaged across different wheat straw varieties (203 spectra)

xylose release (mean values of 0.42, 0.23 and 0.19 g g<sup>-1</sup> dm for total sugar, glucose and xylose release, respectively). The high-yielding straw samples released approximately double the amount of total sugar in comparison to the low-yielding samples, indicating a substantial span in bioethanol potential. The low standard deviation of the laboratory method (SDL) of 0.024 g g<sup>-1</sup> dm for total sugar, 0.016 g g<sup>-1</sup> dm for glucose and 0.010 g g<sup>-1</sup> dm for xylose indicated that the reproducibility of the HTPH assay was high. Explaining the causes for variability of the ethanol potential, as undertaken by Lindedam et al. [6], was beyond of the scope of this study, but generally speaking, annual variation and the effect of cultivar, site and environment are highly influential.

#### Prediction of sugar release

The different transformation methods of the spectra did not considerably improve the accuracy of the predictions of sugar release (Table 3) and only the first derivative transformation resulted in slightly better predictions than the smoothed and normalised spectra. Both first and second

derivative transformations needed a lower number of components (factors) for the predictions, which indicated that the transformation reduced some information that was of little predictive value (Table 3). In all cases, a fair prediction of the potential total sugar, glucose and xylose release was obtained, and the  $R^2$  (coefficient of determination) values of the predictions for the external validation (EV) data set using the smoothing/normalisation transformation were 0.69 for total sugar, 0.63 for glucose and 0.65 for xylose. The root-mean-square error (RMSE) for the same predictions were 0.030, 0.019 and 0.015 g g<sup>-1</sup> dm, respectively (Table 3, Fig. 2), while the ratio of RMSE<sub>EV</sub> to SDL was 1.25, 1.18 and 1.45. In addition to the low RMSE, the differences between cross-validation and the external validation results were quite small, which indicated that the calibrations were robust. These results proved the potential use of calibrations based on FTIR-PAS for the prediction of sugar release from wheat straw. Considering the wide variation in genetic material and environmental conditions during growth, it is reasonable to assume that the model may be applied to other winter wheat straw materials. Applicability of these calibrations in other types of

**Table 1** Most important absorption bands of the mid-infrared spectra of winter wheat straw

Peak no. in Fig. 1	Wavenumber (cm <sup>-1</sup> )	Vibration	Assignment
1	3380	O-H stretching of bonded and non-bonded hydroxyl groups	Included water <sup>l</sup> ; lignin <sup>e</sup>
2	2920	Asymmetric C-H stretching	Aliphatic methylene <sup>b, e, g, k</sup>
3	2850	Symmetric C-H stretching	
4	1735	Un-conjugated C = O stretching	Xylan (hemicellulose) <sup>a-c, e, f, i, j</sup>
5	1650	O-H bending	Absorbed water <sup>a, i</sup>
		Conjugated C-O stretching	Carboxylates <sup>a, i</sup>
6	1600	Aromatic ring vibration	Lignin <sup>a, c, g, j</sup>
		C = C skeletal vibration	
		C = O stretching	
7	1510	Aromatic ring vibration	Lignin <sup>a, c, d, g, j</sup>
8	1460	C-H deformation	Lignin <sup>a, c</sup> ; xylan <sup>j</sup>
9	1429	C-H deformation	Lignin <sup>a, g, l, j</sup>
		CH <sub>2</sub> scissoring	Crystalline cellulose <sup>b</sup>
10	1370	Symmetric C-H deformation	Crystalline cellulose <sup>k</sup> ; hemicellulose <sup>a, i</sup>
11	1320	C-H vibration	Cellulose, hemicellulose, lignin <sup>a</sup>
		CH <sub>2</sub> wagging	Cellulose, hemicellulose <sup>c</sup>
12	1240	C-O stretching	Xylan (hemicellulose) <sup>a, i</sup>
13	1160	C-O-C asymmetric stretching	Crystalline cellulose <sup>b, j, k</sup> ; hemicellulose <sup>a, h</sup>
14	1111	In-plane ring stretching	Crystalline cellulose <sup>b, h, j</sup>
15	1053	C-O stretching	Crystalline cellulose; hemicellulose <sup>a, b, h, k</sup>
16	898	C-O-C stretching	Amorphous cellulose <sup>k</sup>

<sup>a</sup>Pandey and Pitman [28]<sup>b</sup>Gwon et al. [36]<sup>c</sup>Sills, Gossett [16]<sup>d</sup>Gollapalli et al. [22]<sup>e</sup>Xu et al. [15]<sup>f</sup>Kristensen et al. [18]<sup>g</sup>Merk et al. [42]<sup>h</sup>Corgie et al. [19]<sup>i</sup>Cui et al. [43]<sup>j</sup>Chen et al. [44]<sup>k</sup>Ciolacu et al. [27]

plant biomass have not been tested, but it could be feasible since the right regions of the spectrum, corresponding to compounds relevant to the sugars, were taken into account in the calibrations (see section Analysis of regression coefficients).

A number of other studies have used mid-infrared spectroscopy to predict potential ethanol production from biomass. Gollapalli et al. [22] obtained correlations between glucose yield and the diffuse reflectance infrared Fourier transform (DRIFT) spectra, with  $R^2$  values ranging between 0.65 and 0.71 for the different hydrolysis time points of initial rice straw, while the  $R^2$  values of xylose concentration ranged between 0.47 and 0.50. Sills and Gossett [16] were able to explain a larger fraction of the variation during the prediction of glucose and xylose release in a sample set of 24 pretreated and hydrolysed biomass samples (six different plant materials, four different pretreatments with NaOH) using the fingerprint region

(1800–800 cm<sup>-1</sup>) of the ATR-FTIR spectra obtained. The obtained  $R^2$  values of 0.86 and 0.84 for the glucose and xylose content, respectively, were higher than this study's values of 0.63 and 0.65. However, the RMSE values they obtained were 0.078 g g<sup>-1</sup> dm for glucose and 0.093 g g<sup>-1</sup> dm for xylose release, which are higher than the 0.019 and 0.015 g g<sup>-1</sup> dm, respectively, that were obtained in the present study. The high uniformity in this study's sample set (all the straw samples being wheat straw from a relatively small geographical region) meant that the variation in the sample set was small and supported the lower RMSE values. In addition, the use of an external validation data set in the present study can provide more certainty about the predictive power of the model and eliminate the possibility of an overestimation of  $R^2$  values. Martin et al. [23] developed a model predicting the cell wall digestibility of *Sorghum bicolor* biomass using the fingerprint region (1800–850 cm<sup>-1</sup>) of the obtained ATR-FTIR



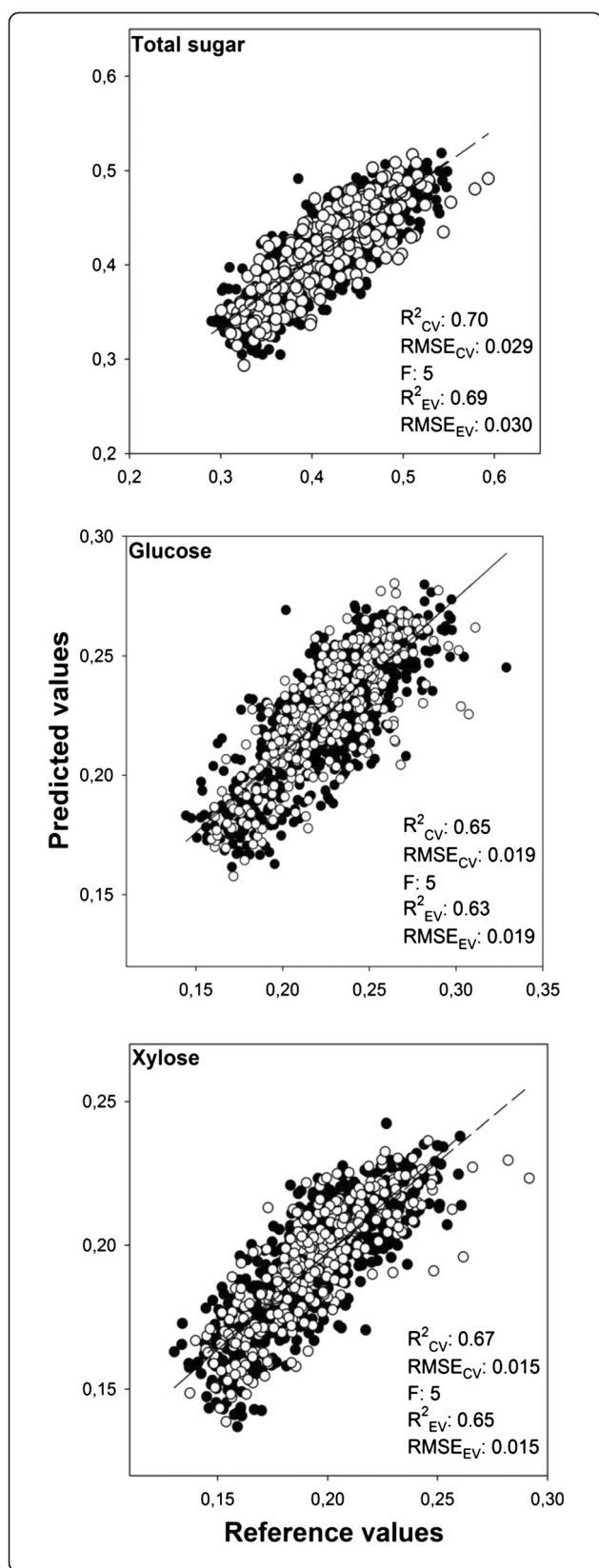


**Fig. 2** Measured vs. predicted values of sugar release. Correlation between reference (measured) and predicted sugar release (in  $\text{g g}^{-1} \text{dm}$ ) in terms of total sugar (glucose plus xylose), glucose and xylose (cross-validation results; black dots, solid regression line, external validation results: white dots, dashed regression line). ( $R^2$  coefficient of determination,  $RMSE$  root-mean-square value,  $CV$  cross-validation data set,  $EV$  external validation data set,  $F$  number of factors used in calibration)

big difference in the  $R^2$  values between calibration and external validation sample sets may indicate the overestimation in the calibration.

NIR spectroscopy has also been used on a number of occasions to predict sugar release or digestibility of biomass samples. Lindedam et al. [12] predicted the sugar release of untreated air-dried wheat straw and achieved  $R^2$  values of 0.56 for the total sugar release, 0.44 for the glucose and 0.69 for the xylose release with  $RMSE$  values of 0.014, 0.010 and 0.005  $\text{g g}^{-1} \text{dm}$ , respectively. Bruun et al. [30] performed partial least squares (PLS) calibration in order to predict the degradability of wheat straw obtaining an  $R^2$  value of 0.72 and an  $RMSE$  of 1.4 % using untreated wheat straw from two different sites. These values are difficult to compare with ours because of different reference methods and sample variability, but they seem to be in the same range and thus indicate that the predictive power of NIR is similar to FTIR-PAS.

A few studies have also been using spectroscopic methods to predict the results of biomass compositional analysis. Tucker et al. [20] applied PLS analysis to develop a model predicting the glucan and xylan content from 35 ATR-FTIR spectra of forest thinning and softwood sawdust (hemlock, Sitka spruce and red cedar). Tamaki and Mazza [21] developed models predicting the glucan and xylan content of wheat and triticale using ATR-FTIR spectra. These studies generally obtained very high predictive power and precision. This may reflect the fact that predictions of the total amount of the specific sugars are easier than predicting the digestible parts. This may be explained by the fact that total cellulose and xylan appears in the spectra as specific bands whereas the digestible amount of the same components depends on a range of other chemical components that may impede the enzymatic hydrolysis of cellulose and xylan.

#### Analysis of regression coefficients

##### Regression coefficients of total sugar prediction

Positive regression coefficients (Fig. 3) were obtained in the region of  $3597\text{--}3440 \text{ cm}^{-1}$  of the spectrum dominated by the stretching vibration of the O-H bond in various compounds, making an interpretation of this region difficult. Nevertheless, Ciolacu et al. [27] suggest that this broad peak is observed in both crystalline and amorphous forms of cellulose, but with a shift towards

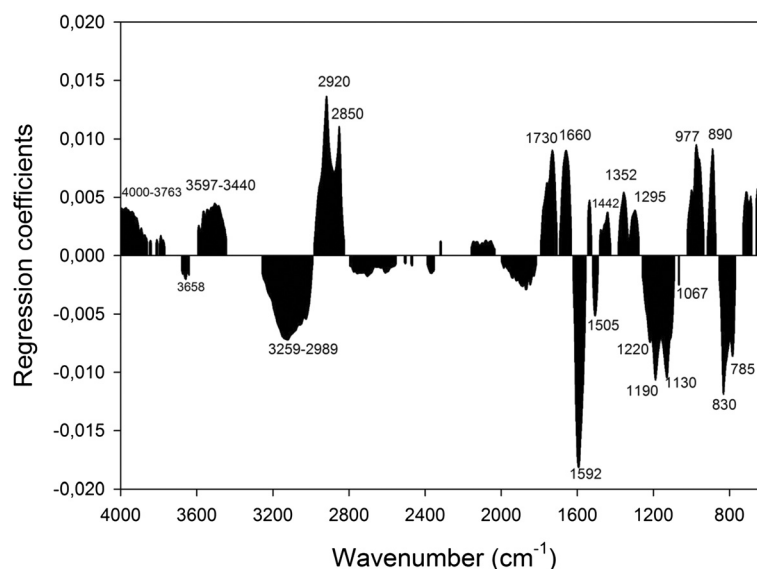


**Fig. 3** Regression coefficients from the prediction of total sugar release. Spectral regions with a significant contribution in the prediction of total sugar release after the pretreatment and enzymatic hydrolysis of wheat straw and during bioethanol production

higher wavenumbers (around 3440 instead of 3350  $\text{cm}^{-1}$ ) for amorphous cellulose. The strong positive association with fermentable sugars, which was observed at 2920 and 2850  $\text{cm}^{-1}$ , corresponds to the aliphatic methylene and is present in the spectrum of amorphous cellulose. The regions at 1730 and 1660  $\text{cm}^{-1}$  are attributed to hemicelluloses and carboxylates. Additionally, a positive association with the sugar release was observed in the regions at 1442 and 1352  $\text{cm}^{-1}$ . According to Liang, Marchessault [31, 32], these regions correspond to the O-H bending in-plane vibration (1442  $\text{cm}^{-1}$ ) and the C-H bending vibration (1352  $\text{cm}^{-1}$ ) of cellulose and hemicellulose. The positively associated region, centred around 1295  $\text{cm}^{-1}$ , can be attributed to  $\text{CH}_2$  wagging [16] in cellulose and hemicellulose or the C-H deformation in hemicelluloses [33]. Finally, both regions at 977 and 890  $\text{cm}^{-1}$  are associated with C-O-C stretching at the  $\beta$ -(1  $\rightarrow$  4)-glycosidic linkages of amorphous cellulose [27]. The interpretation of the positive regression coefficients in this study revealed a strong correlation of sugar release with amorphous cellulose and hemicellulose.

The broad negative associated regions between 3259 and 2989  $\text{cm}^{-1}$  correspond to the O-H stretching vibration of various compounds and, as mentioned earlier, their interpretation is difficult. Fengel [34] asserts that the region of the IR spectrum between 3200 and 3700  $\text{cm}^{-1}$  arises from the intra- and inter-molecular O-H vibrations of crystalline cellulose. The crystalline forms of cellulose appear to be more resistant to enzymatic hydrolysis [35]; therefore, it was expected to be negatively associated with the sugar release. The strongly negatively associated regions at 1592 and 1505  $\text{cm}^{-1}$  are attributed

to lignin, which has been found to play an inhibitory role in the hydrolysis of cellulose and hemicellulose into fermentable sugars [36]. Additionally, the region at 1220  $\text{cm}^{-1}$  can be assigned either to the C-C/C-O stretching vibration in lignin [37] or the C-O-H in-plane bending vibration in crystalline cellulose [38]. Finally, the regions at 1190, 1130 and 1067  $\text{cm}^{-1}$  are associated with crystalline cellulose, while there is not as much information related to the regions under 830  $\text{cm}^{-1}$ . Liang and Marchessault [31] suggested that the regions near 740 and 800  $\text{cm}^{-1}$  are assigned to the  $\text{CH}_2$ -rocking vibration of crystalline cellulose. The interpretation of the negative regression coefficients in this study revealed a negative correlation of sugar release with regions related to lignin and crystalline cellulose. This is not surprising as lignin plays an inhibitory role in the hydrolysis of celluloses and hemicelluloses. Furthermore, the hydrolysis of crystalline cellulose is much slower than amorphous cellulose, as the adsorption of the enzymes necessary for hydrolysis declines with increasing cellulose crystallinity [39].

#### **Regression coefficients of xylose and glucose prediction**

The high correlation ( $r = 0.82$ ) of the measured glucose and xylose yields could mean that the developed calibration model for each sugar monomer might be built on regions of the spectrum determining the other variable. This fact could explain why the same regions of the spectrum were used for the prediction of total sugar, glucose and xylose release (Additional file 1: Figure S1). The division of the calibration set into three smaller subsets led to a decrease in the correlation between the measured glucose and xylose yields from 0.82 in the full



calibration set to 0.37, 0.08 and 0.32 in each of the three subsets, respectively (Fig. 4). The partial least square regression (PLSR) analysis, which was performed on each subset, revealed the spectral regions that were associated with the release of each sugar monomer (Fig. 5).

The differences in the regression coefficients obtained for the prediction of glucose release between the three sample subsets (Fig. 5a) were more obvious than those of xylose (Fig. 5b). Positive regression coefficients at the regions around 2920 and 2850  $\text{cm}^{-1}$  (aliphatics/amorphous cellulose) appeared in all subsets (Fig. 5a), while a positive association with the region at 1670  $\text{cm}^{-1}$  (carboxylates) was present in two of the subsets. The region between 1200 and 1100  $\text{cm}^{-1}$ , which is associated with crystalline cellulose, displayed negative regression coefficients in all subsets, indicating that this region contributed to glucose prediction to a limited extent. Additionally, the region between 1600 and 1500  $\text{cm}^{-1}$  (associated with lignin) displayed negative regression coefficients in two of the subsets. Both regions are therefore related to the restriction of cellulose hydrolysis and consequently, the release of glucose.

In contrast, the regression coefficients obtained for xylose prediction were fairly similar, regardless of which of the three sample subsets was used (Fig. 5b). Xylose release was found to be positively associated with the region around 1740  $\text{cm}^{-1}$  in all subsets and the region around 1250  $\text{cm}^{-1}$  in two of the subsets. Both of them are assigned to the xylans of hemicelluloses, which are built up by xylose monomers and are easily hydrolysable [36].

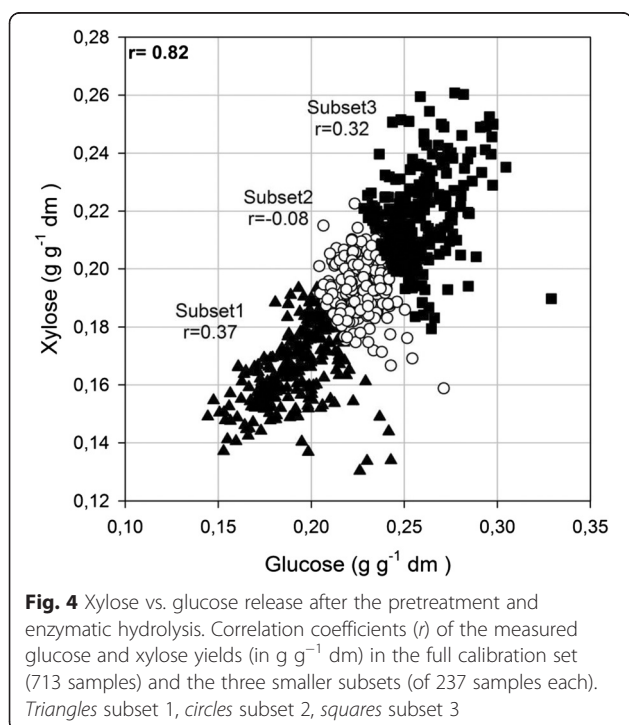


**Fig. 4** Xylose vs. glucose release after the pretreatment and enzymatic hydrolysis. Correlation coefficients ( $r$ ) of the measured glucose and xylose yields (in  $\text{g g}^{-1} \text{dm}$ ) in the full calibration set (713 samples) and the three smaller subsets (of 237 samples each). Triangles subset 1, circles subset 2, squares subset 3

Negative regression coefficients were obtained in the region between 1500 and 1600  $\text{cm}^{-1}$ , which are assigned to lignin. This was expected in all subsets as lignin inhibits the hydrolysis of hemicelluloses.

The regions at 1730 (hemicelluloses) and 970  $\text{cm}^{-1}$  (amorphous cellulose), which were present in the regression coefficients for glucose and xylose prediction, respectively, revealed that some correlation between the two sugar monomers remained, even after subdivision of the calibration set.

## Conclusions

This study established that FTIR-PAS can be used to predict the bioethanol potential from wheat straw and in addition provide structural information on the chemical compounds involved in saccharification. The predictions of total sugar, glucose and xylose release after pretreatment and enzymatic hydrolysis of wheat straw can be characterised as fair (coefficient of determination ranging between 0.64 and 0.70) and accurate (RMSE value ranging between 0.015 and 0.030  $\text{g g}^{-1} \text{dm}$  and RMSE to SDL ratio between 1.18 and 1.45), especially considering the low variability of the sample set in this study caused by the fact that all samples stemmed from mature wheat straw.

The interpretation of the regression coefficients used for the predictions allowed the detection of compounds that contribute to the release of sugars and compounds that do not contribute or even inhibit hydrolysis. As expected, lignin was found to inhibit the hydrolysis of polysaccharides into monomers, while the crystallinity of cellulose might delay its hydrolysis into glucose. On the other hand, amorphous cellulose and xylans were found to contribute significantly to the released amounts of glucose and xylose, respectively.

## Materials and methods

### Sample collection and preparation

A total of 1122 wheat straw samples were collected from nine different locations in Denmark and one location in the United Kingdom (Table 4) from 2006 to 2010. The samples were collected from ongoing experiments with different wheat varieties, fertiliser treatments and harvesting times. The experiments included a total of 203 different wheat varieties. An overview of the origin of samples in terms of experiments, sites and treatments is given in Table 2.

From all but one experiment in Denmark, mature air-dried straw (approximately 7 % moisture) was sampled from the experimental pots after the grain had been harvested by a combine harvester cutting the straw and leaving it in the field. Approximately 80 g of straw was collected representatively from each plot, as described by Lindedam et al. [12] and stored at ambient temperature. Material from the experiment with different harvest times

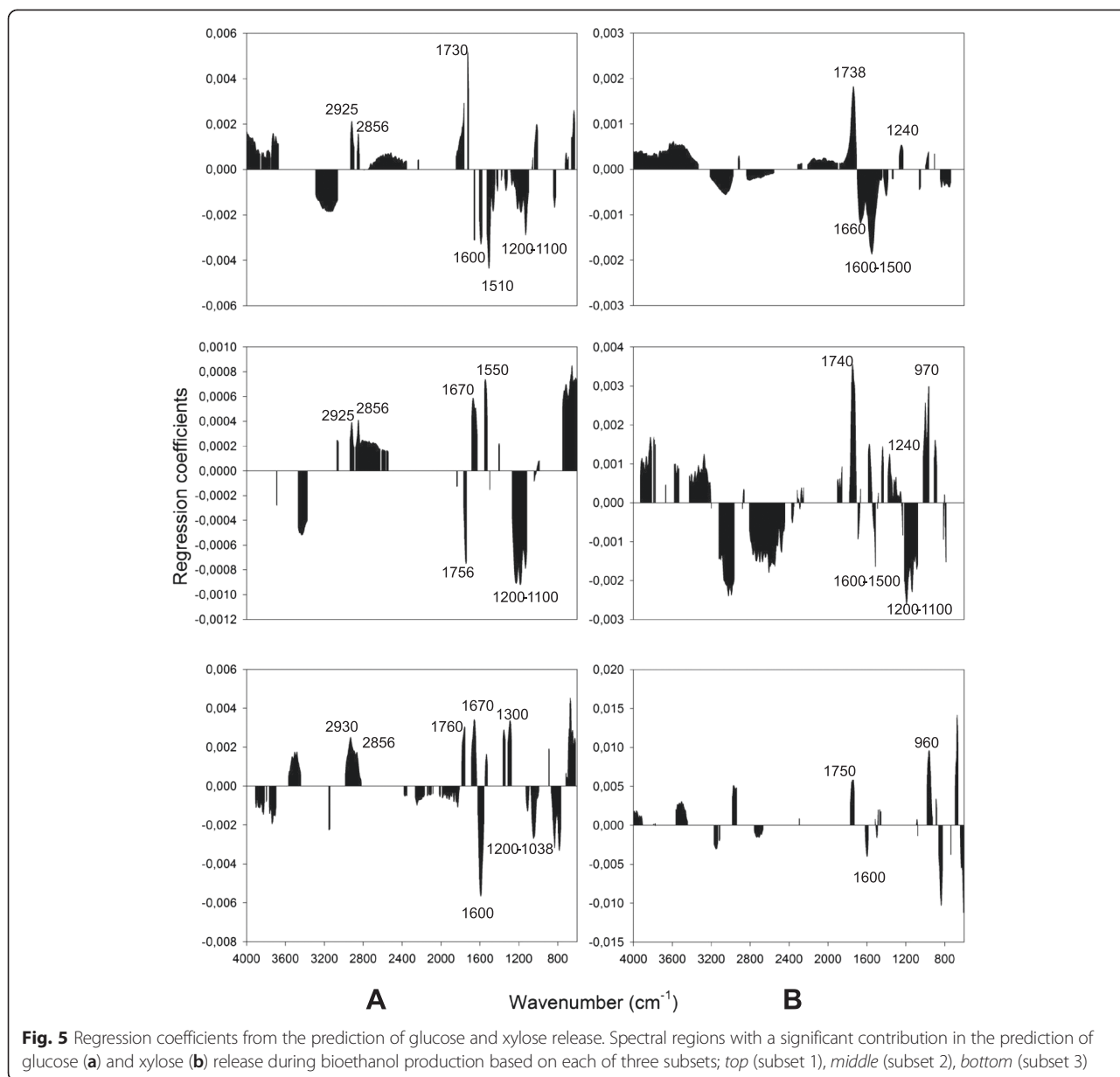


**Table 4** Experiment locations where wheat straw samples has been collected

Site name	Country	Coordinates
Abed	Denmark	54° 49' 40" N, 9° 55' 22" E
Sejet	Denmark	55° 49' 12" N, 11°19' 31" E
Holstebro	Denmark	56° 24' 5" N, 8° 38' 22" E
Tystofte	Denmark	55° 15' 9" N, 11° 20' 14" E
Taastrup	Denmark	55° 40' 36" N, 12° 18' 10" E
Rothamsted	United Kingdom	51° 48' 24" N, 0° 21' 49" W
Søtoften	Denmark	56° 14' 49" N, 10° 6' 1" E
Fyn	Denmark	55° 18' 29" N, 10° 22' 36" E
Hornsherred	Denmark	55° 78' 49" N, 11° 96' 59" E

was collected by hand three weeks before maturity, at maturity and three weeks after. The plants were cut 5–7 cm from the soil, and the grain was removed from the samples before being stored at ambient temperature. Material from the UK was collected as described by Murozuka et al. [40]. Subsequently, all straw samples were ground on a cyclone mill (President, Holbaek, Denmark) mounted with a 1-mm screen.

**Determination of sugar release**

Determination of potential sugar release was carried out at the National Renewable Energy Laboratory (NREL) in Denver, Colorado using a slightly modified method [41] compared to the one described by Selig et al. [9]. Briefly,

2 % dm solids ( $5.0 \pm 0.3$  mg in 250  $\mu$ L of de-ionised H<sub>2</sub>O) were pretreated in triplicate in a 96-well plate in a steam chamber for 17.5 min at 180 °C, with heat-up and cool-down phases of approximately 52 sec and 1.5 min (to reach 120 °C), respectively [9]. Hydrolysis was started by loading total enzyme protein on dry biomass at 70 mg g<sup>-1</sup> dm of Cellic<sup>®</sup> CTec2 (Novozymes, Bagsværd, Denmark). After enzymatic hydrolysis at 50 °C for 70 h, release of glucose and xylose was measured by a glucose oxidase/peroxidase assay and a xylose dehydrogenase assay, respectively (Megazyme International Ireland, Wicklow, Ireland). Total sugars were the calculated values of glucose plus xylose in each sample. Any sugars added with the enzyme mix were accounted for with enzyme-only blanks in every plate.

#### Fourier transform infrared photoacoustic spectroscopy (FTIR-PAS)

No pretreatment of the ground samples was performed prior to the spectroscopic analysis, apart from oven drying at 70 °C for 48 hours. The FTIR-PAS spectra were recorded using a Nicolet 6700 (ThermoScientific, USA) spectrometer equipped with a PA-301 photoacoustic detector (Gaser Ltd, Finland). During the measurement, there was a purging flow with helium gas to reduce the noise caused by moisture evaporating from the samples. The samples were packed in small ring cups of 10-mm diameter and inserted into the PA detector. For each sample, 32 scans in the mid-infrared region between 4000 and 600 cm<sup>-1</sup> at a resolution of 4 cm<sup>-1</sup> were recorded and averaged. Subsequently, the spectra were smoothed by the Savitzky-Golay algorithm [42] using three points on each side (total window of seven smoothing points) and a zero polynomial, and normalised by the mean using The Unscrambler v.10.3 software (CAMO software, Oslo, Norway).

#### Multivariate analysis

PLSR was used to calibrate models predicting glucose and xylose release from the FTIR-PA spectra. Different preprocessing of the spectra were performed in an attempt to obtain better predictions (Table 3). Prior to the PLSR analysis, 54 outliers were removed to increase the model's stability. The selection of the outliers was based on the observation of the Residual vs. Hotelling-T<sup>2</sup> distribution implemented in the software. In order to avoid a possible overestimation, the sample set was divided into a calibration set that contained two thirds of the samples (713 samples) and a smaller external validation set with randomly selected samples from all varieties and sites (355 samples). The calibration set was used to develop calibration models in which the optimal number of components was chosen based on a leave-one segment-out cross-validation using 10 segments of 71 samples. More stable and robust models were achieved by the variable

selection method, known as Martens' uncertainty test [43]. Subsequently, the samples of the external validation set were used to evaluate the robustness of the developed model. The Unscrambler v.10.3 software (CAMO, Oslo, Norway) was used for all calibrations.

After the models had been developed, the regression coefficients were interpreted in order to understand which chemical components were correlated with xylose and glucose release respectively. However, glucose and xylose turned out to be highly correlated ( $r = 0.82$ ). This essentially meant that the regions of the spectrum were not uniquely related to the monomeric sugar that the model was predicting. For example, a model predicting glucose may have high regression coefficients in a region that is related to xylose because xylose is correlated with glucose. In order to be able to identify regions that are uniquely responsible for predicting glucose and not derived from the correlation with xylose, three datasets were produced to reduce the correlation between glucose and xylose. Calibration models were subsequently made predicting glucose and xylose for the data in each of these datasets, and the regression coefficients for these datasets were inspected and interpreted.

The performance of the PLSR-calibrations was determined by the coefficient of determination ( $R^2$ ):

$$R^2 = \frac{\sum_i (y_i - f_i)^2}{\sum_i (y_i - \bar{y})^2}$$

where  $y_i$  represents the observed values and  $f_i$  the predicted values.

The closer the  $R^2$  is to 1, the better the fit of the reference values ( $y_i$ ) to the regression line.

The accuracy of the calibrations was determined by the root-mean-square error (RMSE) (in g g<sup>-1</sup> dm):

$$RMSE = \sqrt{\sum_{i=0}^n (f_i - y_i)^2 / n}$$

In addition, the standard deviation of the laboratory method (SDL) was calculated:

$$SDL = \sqrt{\frac{\sum_{i=1}^n \sum_{j=1}^m (y_{ij} - \bar{y}_j)^2}{m * n - 1}}$$

where  $i$  is the laboratory replicate out of  $m$  replicates and  $j$  is the individual sample out of  $n$  samples.

The closer the ratio of RMSE/SDL is to 1, the better the predictive power of the model to the reference measurements.

## Additional file

**Additional file 1: Regression coefficients from the prediction of glucose and xylose release before the division of the calibration set into three smaller subsets.** Spectral regions with a significant contribution in the prediction of glucose (A) and xylose (B) release during bioethanol production.

### Abbreviations

ATR-FTIR: attenuated total reflection FTIR; DRIFT: diffuse reflectance infrared Fourier transform; EV: external validation; FTIR: Fourier transform infrared; FTIR-PAS: FTIR-photoacoustic spectroscopy; HTPH: high-throughput pretreatment and enzymatic hydrolysis; NIR: near infrared; PLSR: partial least square regression; RMSE: root-mean-square error; SDL: standard deviation of the laboratory method.

### Competing interests

The authors declare that they have no competing interests.

### Authors' contributions

GB performed the FTIR-PAS analysis, the multivariate analysis and drafted the manuscript; SB contributed to the design of the experiment, sample collection, interpretation and the multivariate analysis of the data and the critical revision of the manuscript; JL contributed to the experimental design, sample collection and the interpretation of the obtained data and reviewed the manuscript; SRD and GBT conducted the HTP analysis and contributed to the interpretation of the data and reviewed the manuscript; CP contributed into the multivariate analysis and the interpretation of the obtained spectra and reviewed the manuscript; JM contributed to the conception of the initial experiment and reviewed the manuscript; All authors read and approved the final manuscript.

### Acknowledgements

The research leading to these results has received funding from the People Programme (Marie Curie Actions) of the European Union's Seventh Framework Programme FP7/2007-2013/ in the ReUseWaste project under REA grant agreement n° 289887. This material reflects only the authors' views, and the European Union is not liable for any use that may be made of the information contained therein. The collection of straw was initiated through the OPUS project funded by the Danish Strategic Research Council (grant no. 2117-05-0064). Support for the development of the high-throughput pretreatment and enzyme hydrolysis work was provided by the BioEnergy Science Center. The BioEnergy Science Center is a U.S. Department of Energy Bioenergy Research Center supported by the Office of Biological and Environmental Research in the DOE Office of Science. The National Renewable Energy Laboratory (NREL) is a national laboratory of the US DOE Office of Energy Efficiency and Renewable Energy, operated for DOE by the Alliance for Sustainable Energy, LLC. This work was supported by the U.S. Department of Energy under Contract No. DE-AC36-08-GO28308 with the National Renewable Energy Laboratory.

### Author details

<sup>1</sup>Department of Plant and Environmental Sciences, Faculty of Science, University of Copenhagen, Thorvaldsensvej 40, Frederiksberg C DK-1871, Denmark. <sup>2</sup>National Renewable Energy Laboratory, Biosciences Center, 15013 Denver West Parkway, Golden, Colorado 80401, USA.

Received: 7 April 2015 Accepted: 3 June 2015

Published online: 18 June 2015

### References

- Williams PRD, Inman D, Aden A, Heath GA. Environmental and sustainability factors associated with next-generation biofuels in the US: what do we really know? *Environ Sci Technol*. 2009;43(13):4763–75. doi:10.1021/Es900250d.
- Claassen PAM, van Lier JB, Contreras AML, van Niel EWJ, Sijtsma L, Stams AJM, et al. Utilisation of biomass for the supply of energy carriers. *Appl Microbiol Biot*. 1999;52(6):741–55.
- Kim S, Dale BE. Global potential bioethanol production from wasted crops and crop residues. *Biomass Bioenerg*. 2004;26(4):361–75. doi:10.1016/j.biombioe.2003.08.002.
- Sanchez OJ, Cardona CA. Trends in biotechnological production of fuel ethanol from different feedstocks. *Bioresour Technol*. 2008;99(13):5270–95. doi:10.1016/j.biortech.2007.11.013.
- Sarkar N, Ghosh SK, Bannerjee S, Aikat K. Bioethanol production from agricultural wastes: an overview. *Renew Energy*. 2012;37(1):19–27. doi:http://dx.doi.org/10.1016/j.renene.2011.06.045.
- Lindedam J, Andersen SB, DeMartini J, Bruun S, Jorgensen H, Felby C, et al. Cultivar variation and selection potential relevant to the production of cellulosic ethanol from wheat straw. *Biomass Bioenerg*. 2012;37:221–8. doi:10.1016/j.biombioe.2011.12.009.
- Decker SR, Brunecky R, Tucker MP, Himmel ME, Selig MJ. High-throughput screening techniques for biomass conversion. *Bioenerg Res*. 2009;2(4):179–92. doi:10.1007/s12155-009-9051-0.
- Studer MH, DeMartini JD, Brethauer S, McKenzie HL, Wyman CE. Engineering of a high-throughput screening system to identify cellulosic biomass, pretreatments, and enzyme formulations that enhance sugar release. *Biotechnol Bioeng*. 2010;105(2):231–8. doi:10.1002/bit.22527.
- Selig MJ, Tucker MP, Sykes RW, Reichel KL, Brunecky R, Himmel ME, et al. Original Research: Lignocellulose recalcitrance screening by integrated high-throughput hydrothermal pretreatment and enzymatic saccharification. *Ind Biotechnol*. 2010;6(2):104–11. doi:10.1089/ind.2010.0009.
- Hames BR. High-throughput NIR analysis of biomass pretreatment streams. *Aqueous Pretreatment of Plant Biomass for Biological and Chemical Conversion to Fuels and Chemicals*. John Wiley & Sons, Ltd; 2013. p. 355–68.
- Hames BR, Thomas SR, Sluiter AD, Roth CJ, Templeton DW. Rapid biomass analysis: new tools for compositional analysis of corn stover feedstocks and process intermediates from ethanol production. *Appl Biochem Biotechnol*. 2003;105–108:5–16.
- Lindedam J, Bruun S, DeMartini J, Jorgensen H, Felby C, Yang B, et al. Near infrared spectroscopy as a screening tool for sugar release and chemical composition of wheat straw. *J Biobased Mater Bio*. 2010;4(4):378–83. doi:10.1166/jbmb.2010.1104.
- Hou S, Li L. Rapid characterization of woody biomass digestibility and chemical composition using near-infrared spectroscopy. *J Integr Plant Biol*. 2011;53(2):166–75. doi:10.1111/j.1744-7909.2010.01003.x.
- Stenberg B, Viscarra Rossel RA, Mouazen AM, Wetterlind J. Chapter Five - Visible and near infrared spectroscopy in soil science. In: Donald LS, editor. *Advances in Agronomy*. Academic Press; 2010. p. 163–215.
- Xu F, Yu J, Tesso T, Dowell F, Wang D. Qualitative and quantitative analysis of lignocellulosic biomass using infrared techniques: A mini-review. *Appl Energy*. 2013;104(0):801–9. doi:http://dx.doi.org/10.1016/j.apenergy.2012.12.019.
- Sills DL, Gossett JM. Using FTIR to predict saccharification from enzymatic hydrolysis of alkali-pretreated biomasses. *Biotechnol Bioeng*. 2012;109(2):353–62. doi:10.1002/bit.23314.
- Coates J. Interpretation of infrared spectra: a practical approach interpretation of infrared spectra. In: Meyers RA, editor. *Encyclopedia of Analytical Chemistry*. John Wiley & Sons; 2000. p. 10815–37.
- Kristensen JB, Thygesen LG, Felby C, Jorgensen H, Elder T. Cell-wall structural changes in wheat straw pretreated for bioethanol production. *Biotechnol Biofuels*. 2008;1(1):5. doi:10.1186/1754-6834-1-5.
- Corgie SC, Smith HM, Walker LP. Enzymatic transformations of cellulose assessed by quantitative high-throughput Fourier transform infrared spectroscopy (QHT-FTIR). *Biotechnol Bioeng*. 2011;108(7):1509–20. doi:10.1002/bit.23098.
- Tucker MP, Nguyen QA, Eddy FP, Kadam KL, Gedvilas LM, Webb JD. Fourier transform infrared quantitative analysis of sugars and lignin in pretreated softwood solid residues. *Appl Biochem Biotechnol*. 2001;91–3:51–61. doi:10.1385/Abab:91-93:1-9:51.
- Tamaki Y, Mazza G. Rapid determination of carbohydrates, ash, and extractives contents of straw using attenuated total reflectance Fourier transform mid-infrared spectroscopy. *J Agr Food Chem*. 2011;59(12):6346–52. doi:10.1021/Jf200078h.
- Gollapalli LE, Dale BE, Rivers DM. Predicting digestibility of ammonia fiber explosion (AFEX)-treated rice straw. *Appl Biochem Biotechnol*. 2002;98:23–35. doi:10.1385/Abab:98-100:1-9:23.
- Martin AP, Palmer WM, Byrt CS, Furbank RT, Grof CP. A holistic high-throughput screening framework for biofuel feedstock assessment that characterises variations in soluble sugars and cell wall composition in *Sorghum bicolor*. *Biotechnol Biofuels*. 2013;6(1):186. doi:10.1186/1754-6834-6-186.
- Schmidt K, Beckmann D. Biomass monitoring using the photoacoustic effect. *Sens Actuators B*. 1998;51(1–3):261–7. doi:http://dx.doi.org/10.1016/S0925-4005(98)00229-9.
- McClelland JF, Jones RW, Bajic SJ. FT-IR Photoacoustic spectroscopy. In: Chalmers JM, Griffiths PR, editors. *Handbook of Vibrational Spectroscopy*. John Wiley & Sons; 2002. p. 1–45.

26. Kizil R, Irudayaraj J. Fourier transform infrared photoacoustic spectroscopy (FTIR-PAS). In: Roberts G, editor. *Encyclopedia of Biophysics*: SpringerReference. Berlin Heidelberg: Springer-Verlag; 2013.
27. Ciolacu D, Ciolacu F, Popa VI. Amorphous cellulose-structure and characterization. *Cell Chem Technol*. 2011;45(1–2):13–21.
28. Pandey KK, Pitman AJ. FTIR studies of the changes in wood chemistry following decay by brown-rot and white-rot fungi. *Int Biodeter Biodegr*. 2003;52(3):151–60. doi:10.1016/S0964-8305(03)00052-0.
29. Castillo RD, Baeza J, Rubilar J, Rivera A, Freer J. Infrared spectroscopy as alternative to wet chemical analysis to characterize Eucalyptus globulus pulps and predict their ethanol yield for a simultaneous saccharification and fermentation process. *Appl Biochem Biotechnol*. 2012;168(7):2028–42. doi:10.1007/s12010-012-9915-1.
30. Bruun S, Jensen JW, Magid J, Lindedam J, Engelsen SB. Prediction of the degradability and ash content of wheat straw from different cultivars using near infrared spectroscopy. *Ind Crop Prod*. 2010;31(2):321–6. doi:10.1016/j.indcrop.2009.11.011.
31. Liang CY, Marchessault RH. Infrared spectra of crystalline polysaccharides. 2. native celluloses in the region from 640 to 1700  $\text{Cm}^{-1}$ . *J Polym Sci*. 1959;39(135):269–78. doi:10.1002/pol.1959.1203913521.
32. Marchessault RH, Liang CY. Infrared spectra of crystalline polysaccharides. 8. Xylans. *J Polym Sci*. 1962;59(168):357–78. doi:10.1002/pol.1962.1205916813.
33. Kaushik A, Singh M. Isolation and characterization of cellulose nanofibrils from wheat straw using steam explosion coupled with high shear homogenization. *Carbohydr Res*. 2011;346(1):76–85. doi:10.1016/j.carres.2010.10.020.
34. Fengel D. Characterization of cellulose by deconvoluting the OH valency range in FTIR spectra. *Holzforschung - International Journal of the Biology, Chemistry, Physics and Technology of Wood*; 1992. p. 283.
35. Beguin P. Molecular biology of cellulose degradation. *Annu Rev Microbiol*. 1990;44:219–48. doi:10.1146/annurev.mi.44.100190.001251.
36. Perez J, Munoz-Dorado J, de la Rubia T, Martinez J. Biodegradation and biological treatments of cellulose, hemicellulose and lignin: an overview. *Int Microbiol*. 2002;5(2):53–63. doi:10.1007/s10123-002-0062-3.
37. Kubo S, Kadla JF. Hydrogen bonding in lignin: a Fourier transform infrared model compound study. *Biomacromolecules*. 2005;6(5):2815–21. doi:10.1021/bm050288q.
38. Gwon JG, Lee SY, Doh GH, Kim JH. Characterization of chemically modified wood fibers using FTIR spectroscopy for biocomposites. *J Appl Polym Sci*. 2010;116(6):3212–9. doi:10.1002/App.31746.
39. Yang B, Dai Z, Ding S-Y, Wyman CE. Enzymatic hydrolysis of cellulosic biomass. *Biofuels*. 2011;2(4):421–49. doi:10.4155/bfs.11.116.
40. Murozuka E, Laursen KH, Lindedam J, Shield IF, Bruun S, Magid J, et al. Nitrogen fertilization affects silicon concentration, cell wall composition and biofuel potential of wheat straw. *Biomass Bioenerg*. 2014;64:291–8. doi:10.1016/j.biombioe.2014.03.034.
41. Lindedam J, Bruun S, Jorgensen H, Decker SR, Turner GB, DeMartini JD, et al. Evaluation of high throughput screening methods in picking up differences between cultivars of lignocellulosic biomass for ethanol production. *Biomass Bioenerg*. 2014;66:261–7. doi:10.1016/j.biombioe.2014.03.006.
42. Savitzky A, Golay MJE. Smoothing and differentiation of data by simplified least squares procedures. *Anal Chem*. 1964;36(8):1627–39. doi:10.1021/Ac60214a047.
43. Martens H, Martens M. Modified jack-knife estimation of parameter uncertainty in bilinear modelling by partial least squares regression (PLSR). *Food Qual Prefer*. 2000;11(1–2):5–16. doi:10.1016/S0950-3293(99)00039-7.
44. Chen H, Ferrari C, Angiuli M, Yao J, Raspi C, Bramanti E. Qualitative and quantitative analysis of wood samples by Fourier transform infrared spectroscopy and multivariate analysis. *Carbohydrate Polymers*. 2010;82:772–8.

**Submit your next manuscript to BioMed Central and take full advantage of:**

- Convenient online submission
- Thorough peer review
- No space constraints or color figure charges
- Immediate publication on acceptance
- Inclusion in PubMed, CAS, Scopus and Google Scholar
- Research which is freely available for redistribution

Submit your manuscript at  
[www.biomedcentral.com/submit](http://www.biomedcentral.com/submit)

